Microelectronic Engineering 209 (2019) 20–27

Contents lists available at ScienceDirect

Microelectronic Engineering

journal homepage: www.elsevier.com/locate/mee

Research paper

An electro-kinetic platform based on printed circuit Board technology for identification and characterization of biological cells

Reda Abdelbaset[a,b,*], Marwan Abouelalla[b], Yehya H. Ghallab[a,b,c], Hamdy Abdelhamid[b], Yehea Ismail[b]

[a] Biomedical Engineering Department, Helwan University, Cairo, Egypt
[b] Center of Nano electronics and Devices (CND), Zewail City of Science and Technology and The American University in Cairo (AUC), Cairo, Egypt
[c] Electronics and Communication Engineering Department (ECE), Kuwait College of Science and Technology, Kuwait

ARTICLE INFO

Keywords:
Dielectrophoresis
Traveling
Electro-rotation
Levitation
PCB
Microbeads

ABSTRACT

This paper presents an electro-kinetic platform that combines three DEP configurations based on printed circuit board (PCB) technology. These configurations are: traveling, rotation and levitation DEP. The strength and effectiveness of the generated electric field of traveling and levitation configurations are simulated using COMSOL Multiphysics ®. The proposed platform is experimentally tested using microbeads (Carboxyl Polystyrene particles) in order to evaluate its performance. Also, the efficiency and functionality of the proposed platform when subjected to different waveform of signals (sine wave, and square wave) are presented and discussed. Moreover, the proposed platform can be used to extract other features of the biological cells, such as capacitance and permittivity.

1. Introduction

The separation and manipulation techniques of biological particles became the focus of scientists in various fields such as engineering, chemistry, medicine, physics and biology. The electrical characteristics and dielectric properties play important roles in characterization and separation of biological particles such as normal and abnormal cells [1]. The dielectrophoresis (DEP) is a phenomenon in which a non-uniform electric field generates a force on neutral but polarizable particles [2–4]. The DEP electro-kinetic is the manipulation of polarizable particles as a result of the interaction between a non-uniform electric field and the particles. DEP is preferred for separation and manipulation of biological particles due to several advantages i.e. its high sensitivity in detection of cells which have different dielectric properties, and it does not need large volume of samples and any expensive reagents compared to other techniques [5,6].

However, Based on DEP configuration at specific frequencies, it is possible to distinguish between different types of biological cells, where, the direction and the amplitude of the acquired angular velocity by the biological cells can vary [7]. Generally, DEP based electro-kinetic may include three major configurations, they are traveling wave dielectrophoresis (twDEP), DEP electro-rotation (rotDEP) and DEP levitation (levDEP) which are widely used techniques for manipulation and separation of biological cells. twDEP is a widely used technique for particle manipulation and separation. The twDEP is obtained by a non-uniform electric field which is generated by applying a sequence of 90° phase shifted [0° 90° 180° 270°] signals to microelectrode array. Morgan et., al. used Fourier series analysis to simulate the electric field that is generated by a parallel bar electrode array for two cases: a two-phase and a four-phase configuration [8]. Bunthawin et., al. presented a microchip based on twDEP configuration to estimate the dielectric properties of yeast [9]. Cheng et., al. demonstrated a high throughput continuous bio-particle sorter based on 3D traveling-wave dielectrophoresis (twDEP) at an optimum AC frequency of 500 kHz [10].

Also, rotDEP is a phenomenon for characterization and identification of biological particles. The rotDEP force is achieved by applying a rotating electric filed using four 90° phase shifted [0° 90° 180° 270°] signals. Hang et., al. measured the dielectric properties (rotation speeds) of cells by an effective electrorotation technique [11].

levDEP is not only able to characterize the biological particles based on the variations in levitation height but, also it is capable of trapping biological particles for other tests to be implemented [12]. The levDEP force is achieved when a cone shaped non-uniform electric field is generated (i.e., weak area of electrical field strength compared to the surrounding area is generated).

DEP phenomenon is achieved through a specific microelectrodes

* Corresponding author at: Biomedical Engineering Department, Helwan University, Cairo, Egypt.
E-mail address: reda.mohamed@aucegypt.edu (R. Abdelbaset).

https://doi.org/10.1016/j.mee.2019.02.001
Received 14 October 2018; Accepted 9 February 2019
Available online 09 March 2019
0167-9317/

array that can be implemented by various techniques such as Complementary metal–oxide semiconductor (CMOS) technology and PCB technology. Cen et., al. showed an Integrated Circuit (IC) that integrated the three electrokinetic techniques onto a single chip which is fabricated using a conventional CMOS process [13]. In [14], a microfluidic platform on chip is reported for trapping, counting and detecting S. oneidensis cells. Morganti et., al. designed a microdevice coated with titanium dioxide for separation and manipulation of cells [15]. Hasan et., al. implemented a negative AC dielectrophoretic investigations using elliptic electrode geometry based on PCB technology [16]. Altomare et., al. created a software-controlled platform based on PCB technology for trapping cells [17]. Ho et., al. fabricated a simple microfluidic system using printed circuit board for manipulating microbeads [18]. The PCB technology has many advantages such as low cost, widely available, re-workable and excellent shelf life [19]. The previous works using PCB technology focused on a single configuration (traveling DEP). However, in this work, an integrated system is preferred and implemented that combines the three major configurations (traveling, rotation, and levitation). The advantages of the proposed platform can be summarized as follows: 1) Reduce the required fabrication area and consequently the cost. In other word, the two configurations (i.e., rotation and traveling) are fabricated with merged circles. 2) Decrease the required number of samples and testing time. So, the two features (i.e., rotation and levitation) are combined to use only one sample for both tests Furthermore, this combination based on PCB technology is proposed to extract different dielectric features to get a highly efficient identification and characterization. Many physical properties of different biological cells can be extracted by the electrokinetic platform which help in separating between different types and states of cells (i.e., Normal, and lesions) [12]. The microbeads are plastic microsphere widely used in cosmetics and personal care products as well as biomedical and health science research [20]. In this work, microbeads are used to emulate live biological cells which are both simulated using COMSOL and experimentally tested within the platform.

2. DEP'S theory

DEP differs from the conventional electrophoresis, where a non-uniform electric field is required to achieve the DEP force. Electro-kinetics broadly is the motion of polarizable particles immersed in a fluid as a result of an applied nonuniform electric field [1]. The governing vector relationship defining the DEP force is $FDEP = (\rho \cdot \nabla)E$, where ρ is the effective polarization induced in the particle, ∇ is the gradient operator and E is the intensity of a non-uniform electric field [12]. Table 1 shows the DEP forces equations for the three major configurations (i.e., Eqs. (1)–(3) show twDEP force [6,21], Eq. (4) shows rotDEP force [11], and Eqs. (5), and (6) show levDEP force [12,22]). However, each configuration will be described in detail in the next sections.

3. The proposed electro-kinetic electrodes

Fig. 1 shows the layout of the proposed electro-kinetic electrode which combines three DEP configurations (twDEP, rotDEP, and levDEP). The platform has four groups of electrodes with homogenous geometry (T, R, QR and L) as shown in Fig. 1. Where, (T) refers to the traveling group that consists of 32 electrodes. (R) refers to rotation group that consists of four subgroups, where, each one consists of 31 electrodes. QR refers to quadrupole rotation that consists of four squares. Finally, L refers to quadrupole levitation that consists of four squares. The twDEP electrodes can be implemented using one of the following shapes: - 1) a concentric ring structure [13] as shown in Fig. 1. 2) A planar linear interdigitated array [23,24]. The concentric rings micro-electrode design has several advantages over other designs [24]; therefore, it is preferred for twDEP configuration.

Table 1
The DEP equations of the three major configurations.

	Equation
1	Travelling $F_{twDEP} = \frac{-4\pi\varepsilon_m R^3 E_{0(rms)}^2 Im([Ke])}{\lambda}. \hat{r}_0$ (1), ε_m ➔ the relative permittivity of the surrounding medium, R ➔ the radius of particle, E_0 ➔ the nonuniform electric field, λ ➔ is the wavelength imposed by the center-to-center electrode spacing plus the electrical phasing, Im ➔ the imaginary part, [Ke] ➔ the Clausius-Mossotti factor (CM factor). $Ke(\omega) = \frac{\varepsilon_p^* - \varepsilon_m^*}{\varepsilon_p^* + 2\varepsilon_m^*}$ (2), $\varepsilon_p^* = \varepsilon_p - \frac{i\sigma_p}{\omega}$, $\varepsilon_m^* = \varepsilon_m - \frac{i\sigma_m}{\omega}$ (3), ε_p, ε_m ➔ the permittivity of particle and medium, σ_p, σ_m ➔ the conductivity of particle and medium, ω ➔ the angular frequency of the electric field,
2	Electrorotation $FDEP = 2\pi\varepsilon_m R^3 \, Re \, [Ke] \nabla E^2$ (4),
3	Levitation $P = 4\pi\varepsilon_m R^3 KeE$ (5), $T = -4\pi\varepsilon_m R^3 \, Im \, [Ke] E^2$ (6).

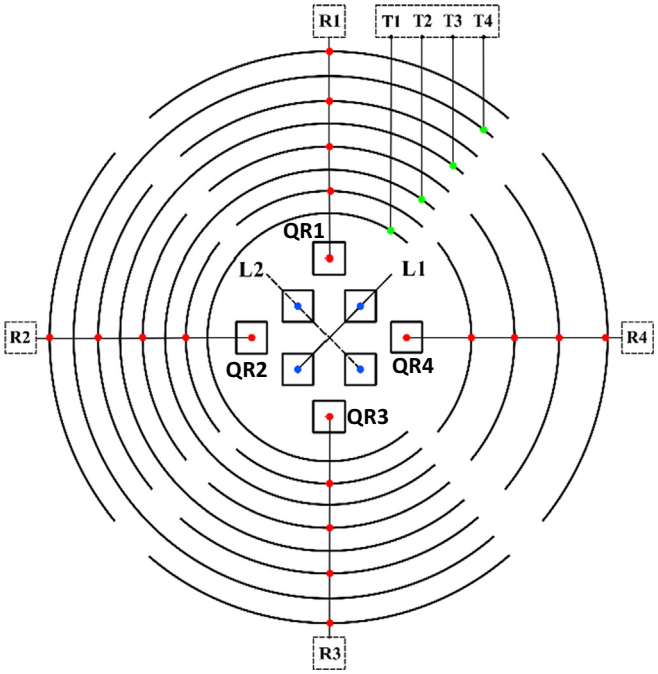

Fig. 1. A Simple layout of four electro-kinetic configurations. The traveling and the electro-rotation array are represented by concentric rings, while, squares represent the quadrupole levitation configuration and the quadrupole electro-rotation configuration.

The levDEP electrodes are classified into three types, they are 1): a cone plate levitation system, 2) Ring dipole levitation system, and 3) a quadrupole levitation system [12]. The first configuration is complex to be implemented based on PCB technology because of the cone shape and the adjustment of ground plate at very near distance [12]. Similarly, the second configuration needs ground plate at a near distance from ring planar and resistors between each two successive rings to permit applying gradient electric potential, therefore, it is complex to be implemented based on PCB technology [12]. Consequently, the quadrupole design is preferred to generate the desired non-uniform electric field pattern [22]. The rotDEP configuration is implemented based on a four poles model, where these four poles generate a rotating

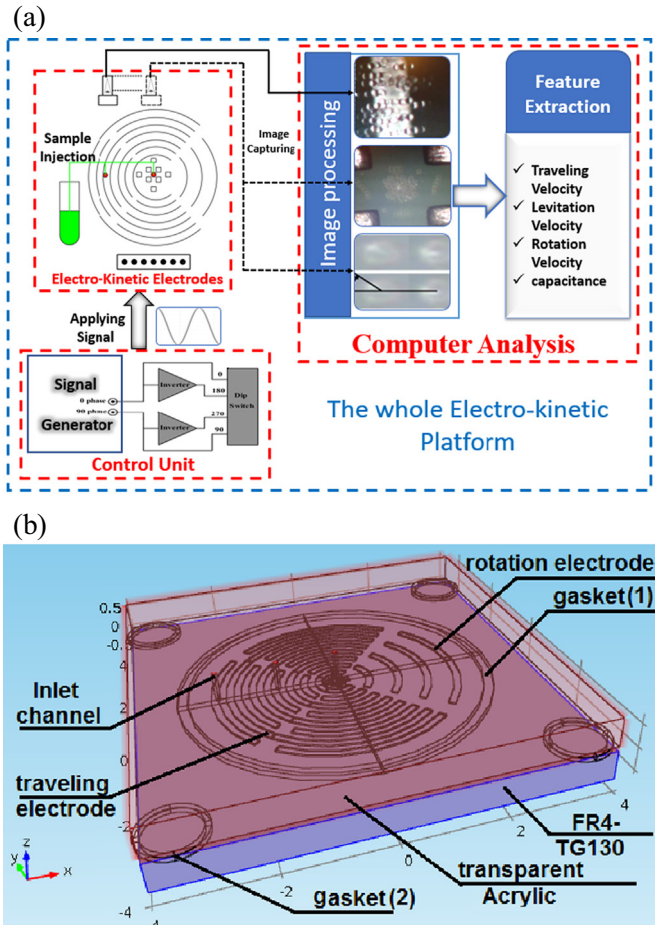

Fig. 2. a) The block diagram of whole system, b) The proposed microfluidic chamber.

electric filed that will allow the cells to rotate as well. Different shapes are previously presented and used, such as, concentric rings configuration [13], octode [8], arrows (quadrupole and octupole) [25]. The proposed electro-rotation electrodes are implemented using concentric rings for being compatible with the configuration of traveling microelectrodes. Furthermore, the concentric ring configuration is supported by quadrupole electrodes to increase the intensity of a rotating electric field at the center of electro-kinetic platform at which the sample is inserted.

4. The proposed platform

Fig. 2(a) shows the testing flow and the block diagram of each part of the proposed electrokinetic platform. it consists of the following parts: 1) Electrodes and chamber, 2) Control unit [function generator, signal amplifying and inverting, and switching system), 3) microscope and camera, and 4) computer. From Fig. 2(a) the working flow of the proposed platform is shown. It starts by injecting a sample to be tested, then, applying an electrical signal, and recording a video of the cell movement. Finally, the recorded video is analyzed to extract the results (i.e., traveling speed, levitation speed, angular speed, and capacitance).

4.1. Electrode configuration

The proposed electrodes were fabricated using the immersion silver process of PCB technology. Unlike other techniques this process has several advantages such as low cost compared to gold immersion, also, silver is suitable to keep the biological cells alive during the test [26].

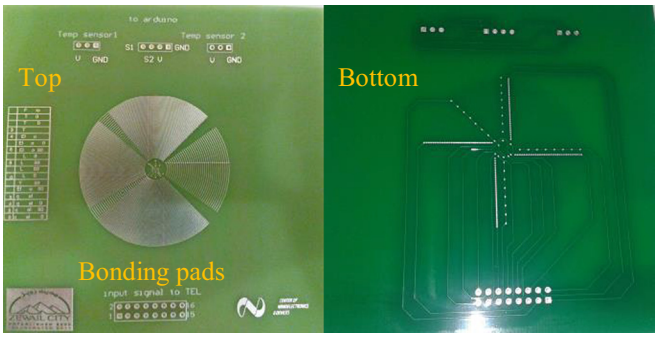

Fig. 3. A photograph of the fabricated top layer of the proposed Electro-kinetic platform.

Fig. 3 shows the fabricated two layers PCB (platform). The top layer: includes the electro-kinetic microelectrodes, while, the bottom layer: includes the physical connections between the electrodes and the pads. The bottom layer is covered by a green mask to protect connections from damage and any external metal that may cause short circuit. Also, there are 16 bonding pads used to connect the electrodes to the external control circuit (4 pads per each group). All groups were connected to their related pads via traces within the bottom layer of the PCB. Each concentric ring has a 150 μm width and a 150 μm space between two successive rings. These dimensions are chosen to accommodate the fabrication constraints. The electrode thickness is 1 oz. (34.79 μm). The total size of the platform is 10.16 × 10.16 cm^2.

4.1.1. Electrodes for twDEP configuration

The twDEP configuration is achieved using the concentric ring groups T1 to T4 as shown in Fig. 1. Each group consists of eight rings that are connected to one bonding pad; therefore, the total bonding pads for twDEP configuration are four pads. Each concentric ring has 150 μm width and 450 μm space between two successive rings. The radius of the first ring is 3.302 mm. The phase shift of the applied signals to T1–T4 electrodes are 270° 180° 90° 0°, respectively.

4.1.2. Electrodes for electro-rotation

The concentric ring sectors R1 to R4 are used for rotDEP configuration as shown in Fig. 1. Each sector consists of 31 concentric rings that are connected to one bonding pad, consequently, the total bonding pads for electro-rotation configuration are four pads. Each concentric ring has 150 μm width and 450 μm space between two successive rings. The radius of the first ring is 3.6068 mm. The sectors R1 to R4 are excited by externally applied signals in the phase order [0° 90° 180° 270°] respectively. The efficiency of rotDEP configuration is enhanced by using planar quadrupole electrodes. As, there are four squares in order to increase the intensity of the electric field at the center of the platform. The size of each square is 381 μm × 381 μm, as shown in Fig. 1. The four quadrupole electrodes are excited by externally applied signals in the phase order [0° 90° 180° 270°], respectively.

4.1.3. Electrodes for levitation

Four planar squares (quadrupole microelectrodes) are used for levDEP configuration. The size of the squares is 100 μm × 100 μm and there is a 100 μm space between the squares as shown in Fig. 1. The quadrapole microelectrodes are supplied by signals with 0° phase shift on two opposite squares (L2) and 180° phase shift on the other opposite squares (L1) as shown in Fig. 1.

4.1.4. Microfluidic chamber

The microfluidic chamber plays an important role in controlling the location of the inserted sample, as well as the exit location of the sample after finishing the test. Thus, it should have specific conditions, such as: the chamber needs to be transparent and has inlet channels for different

DEP force types. The proposed microfluidic chamber consists of three components, they are: 1) the body which is fabricated from a high-quality transparent acrylic. 2) inlet channels which include three inlet channels at specific locations on the platform, each inlet is used for a specific DEP configuration (i.e., traveling, rotation and levitation DEP), as shown in Fig. 2(b), and 3) Gaskets: The chamber is separated by a specific distance from the main platform by two types of gaskets; large gasket which is placed around the electrodes. It keeps the sample at the targeted location and prevents it from spreading out on the platform. Small gaskets are placed at the corners, refer to Fig. 2(b).

4.2. Control unit

4.2.1. Source of applied signal

A function generator is used to produce sine and square wave signals with different phase angles (0° and 90° phase shift). The other two signals (180° and 270° signals) are generated by an electronic circuit that will be presented in Section 4.2.2 as shown in Fig. 2(a). The amplitude of the applied signal for all tests is 10Volt.

4.2.2. Control circuit

An inverting amplifier is used (current conveyer (AD844)) to generate 180° and 270° phase shifted signals from 0° and 90° phase shifted signals, respectively. Therefore, the available generated signals are [0° 90° 180° 270°]. The output of each inverting circuit is tested using an oscilloscope to ensure the functionality of the circuit. Finally, DIP (dual in line package) switch is used in selection of the targeted DEP force configuration. Also, the DIP switch is used to control the input signals for the selected configuration.

4.3. Microscope and camera

An optical microscope (Olympus) with digital camera is used to monitor and record the DEP based experiments as shown in Fig. 2(a).

4.4. Computer

A computer is connected to the digital camera in order to record videos for different configurations. These videos are analyzed to extract the velocities of the cells [27] as shown in Fig. 4. An open source video analysis and modelling tool is used to measure the traveling speed, and the rotation speed of the microbeads. The traveling speed is measured as follows: 1) capture videos for the microbeads translation, 2) define the coordinate axes and calibration stick (using scale bar), and the frame rate per second for the video, 3) manually track the translation of beads, 4) export the velocities of different samples, then compute the average and up/down error. Similarly, the rotation speed of microbeads is measured, but increases these steps, before tracking the image is focused on particle. Then, the coordinate system is linked with the centre of mass of particle in order to remove the effect of particle motion.

5. Finite element model of the electrodes

COMSOL Multiphysics 5.3 is used to model and simulate the electrokinetic platform (concentric ring for traveling, and quadruple levitation), as shown in Fig. 5. The model procedure is as follows: 1) pre-processing; includes the selection of space dimensions, suitable physics for applying the electric field and the appropriate study related to an interested parameter (i.e. time or frequency or stationary). 2) Geometry: the structure of the model is built. 3) Materials: the material type of each part of the model is defined. 4) Loads and Conditions: specific physics such as electric potential, creeping flow, and particle tracing for fluid flow is applied. 5) Meshing: the structure is divided into small elements with specific size and shape [28].

Fig. 5(a, and b) show both the COMOSOL input file for twDEP and

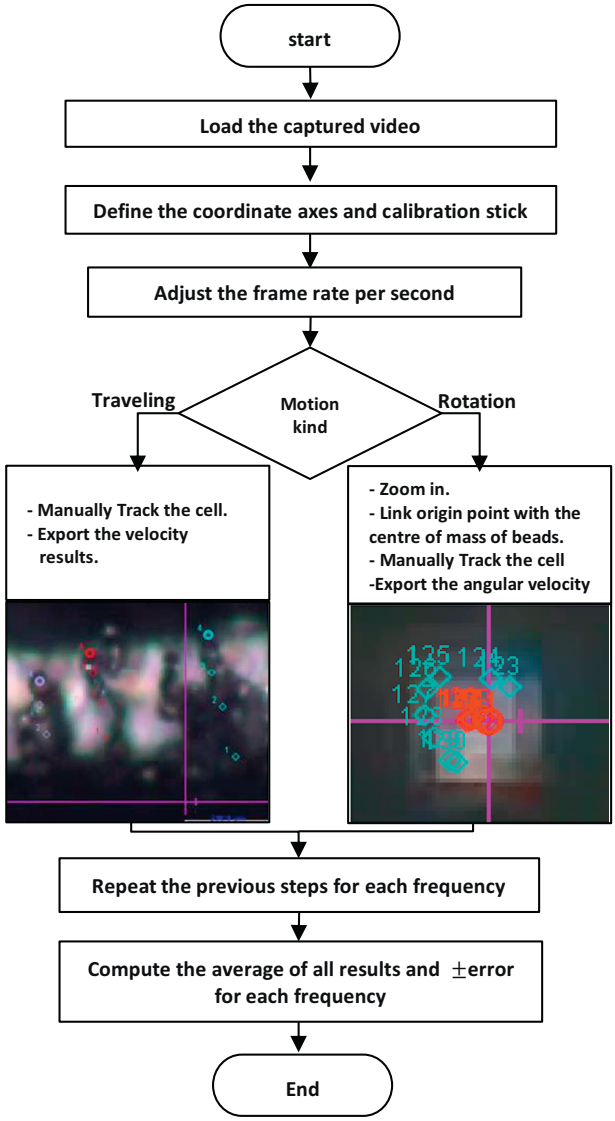

Fig. 4. Flow chart of the captured videos analysis using Tracker program.

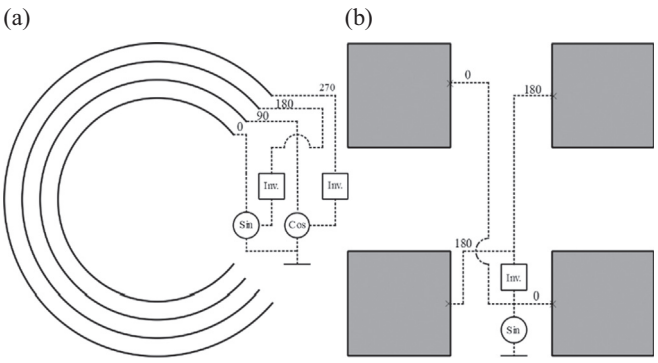

Fig. 5. a) A schematic of traveling concentric rings configuration and the appropriate applied signal for DEP traveling, and b) A schematic of quadrupole levitation configuration.

levDEP configurations, respectively. The distance between the four squares of the levDEP configuration is 100 μm and the pitch is 100 μm as well, refer to Fig. 5B.

For traveling concentric rings configuration, the applied voltage is 10 V_{pp} and 100 kHz sine wave or square wave with four different phase

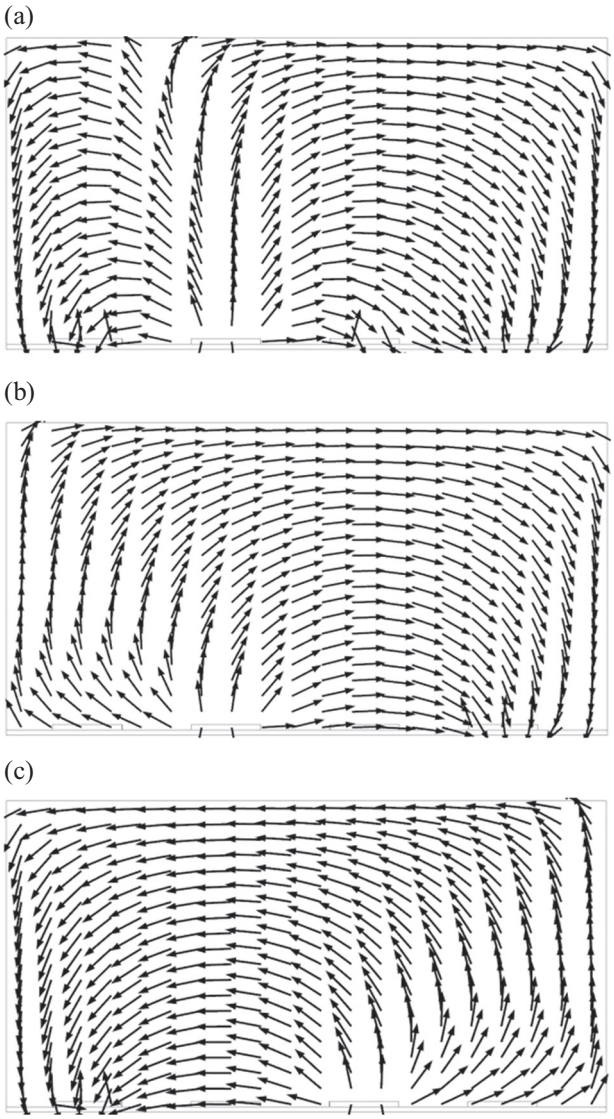

Fig. 6. The arrows describe the distribution of electric field which is generated by sequence of electrical potential with phase shift: a) [0 90 180 270], b) [90 270], and c) [0 180].

shift values (0°, 90°, 180° and 270°), as shown in Fig. 5(a). For quadrupole levitation configuration, the applied voltage is 10 V_{pp} and 100 kHz sine wave or square wave with two out of phase signals are applied on the electrodes, as shown in Fig. 5(b).

6. Simulation and experimental results

6.1. Simulation results

The proposed platform (twDEP, and levDEP configurations) is simulated using COMSOL multi-physics, in order to simulate the produced electric field, and the induced kinetic energy in particles for both twDEP and levDEP configurations. The electrodes shown in Fig. 5 are subjected to different sequence of electric signals with different phase shifts. Fig. 6 shows samples of the electric field profile for (0°, 90°, 180° and 270°), (90° and 270°) and (0° and 180°), respectively.

6.2. Experimental results

In this section, the previous simulation results are confirmed by the experimental work to prove the functionality of the proposed platform,

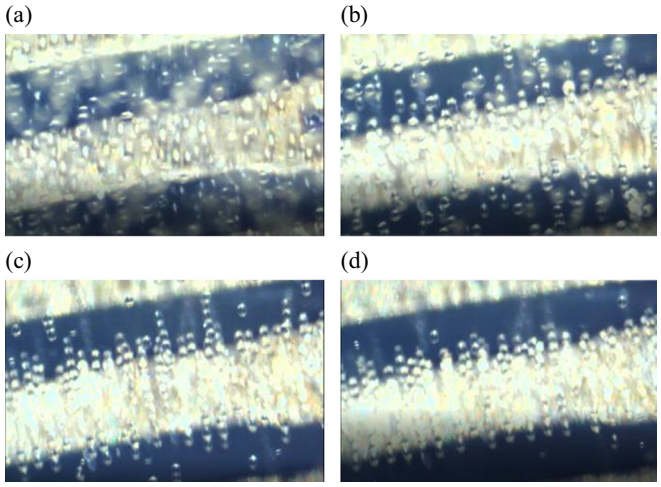

Fig. 7. a) the random spread of microbeads before turning on electric field, b) the levitation component of twDEP of microbeads, c), and d) the alignment and the translation back and forth of the microbeads under effect of twDEP force.

i.e. the ability to manipulate cells with high efficiency. The diameter of the used microbeads is 20 μm. The concentration of microbeads is 2.2% w/v, and the storage buffer is deionized water with 0.02% Sodium Azide.

6.2.1. twDEP configuration

Fig. 7 shows snapshots of the microbeads under the effect of the twDEP force at different time. Fig. 7(a) displays the initial spread of microbeads on the microelectrodes before turning on the electric field. In Fig. 7(b), the microbeads became more precise, bright, and clear, because it positioned in the focus of the microscope. Consequently, this describe the levitation of microbeads before traveling under the effect of the DEP force after turning on the electric field [6]. Fig. 7(c, and d) show the alignment and movement back and forth of the microbeads under the effect of the twDEP force. In other word, the direction of traveling is reversed by changing the applied signal from sine wave sequence [0 90 180 270] to [0 180] sequence and vice versa.

6.2.2. Quadrupole levitation configuration

Fig. 8 shows snapshots of the microbeads under the effect of levDEP force at different time. Fig. 8(a) shows the initial spread of microbeads over the microelectrodes before turning on the electrical signals. While, Fig. 8(b–d) show the levitation of microbeads after turning on an ac signal at different frames until it trapped and levitated at the center.

6.2.3. Dual electro-rotation configuration

Fig. 9 displays snapshots of the microbeads under the effect of rotDEP force at different time. The rotation of the beads is monitored by following a marked high intensity point which made by the reflection of the microscope's light on the PCB. Fig. 9(a) and (b) show the assumed initial angle of a rotated microbead particle, where, (b) the focused of (a). While, Fig. 9(c) shows the second angle of a rotated particle after 0.264 s from turning on ac sine wave signal, and Fig. 9(d) shows the focused of (c).

7. Discussion

Fig. 10 shows the measured velocities with respect to frequency for both DEP configurations (twDEP and rotDEP). From Fig. 10(a), it can be seen that the twDEP velocity of the manipulated beads is linearly increased with the increase of the frequency of the applied signal to reach the highest value at 800 kHz. After 800 KHz, the speed is decreased with increasing the frequency. Similarly, Fig. 10(b) shows that the peak

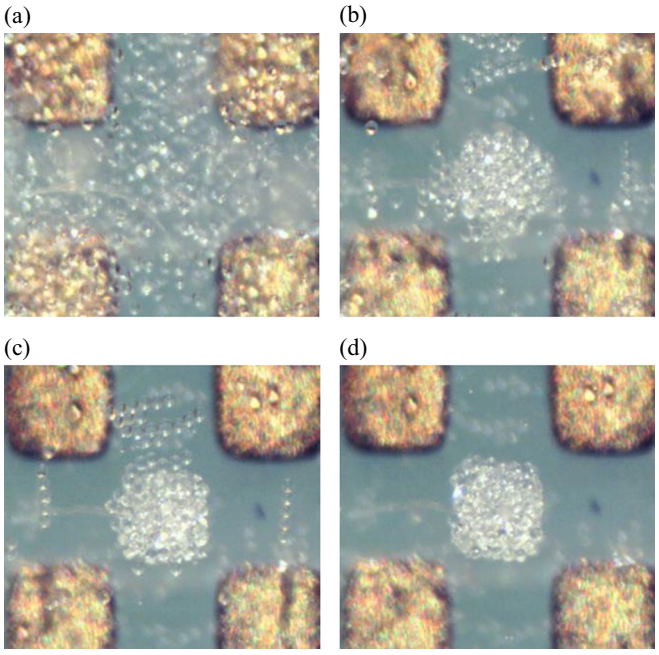

Fig. 8. Screen shots of microbeads spread at different times under effect of levDEP, (a) before turning on square electric potential. b)–d) the trapping of microbeads after turning on square wave electric potential.

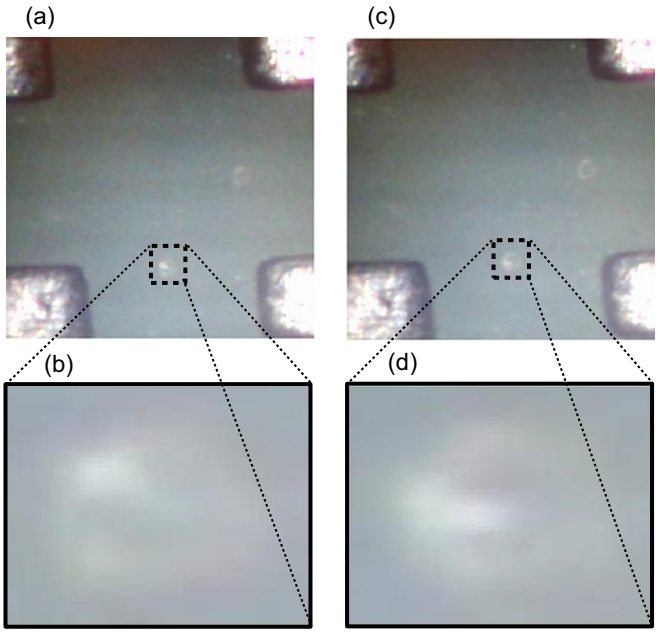

Fig. 9. a–c) Snap shots with different angles of rotation of microbeads under effect of electro-rotation configuration. b, d) the focused of a, and c, respectively.

of the rot DEP velocity is reached at 800 KHz (i.e., the first characteristic peak is at 800 KHz). It is noteworthy that the microbeads rotated in the opposite direction (clockwise) at 500 KHz, although, the rotation of microbeads at the rest of the frequencies in the anticlockwise direction. Fig. 11(a, and b) present the simulation results of the induced particles' (microbeads) kinetic energy under the effect of both sinusoidal and square wave signals for the twDEP, and levDEP configurations. From Fig. 11(a, and b), it can be noticed that the square wave signal induces higher kinetic energy in particles compared to the sinusoidal signal [29]. This result is in good agreement with the fact that the square wave

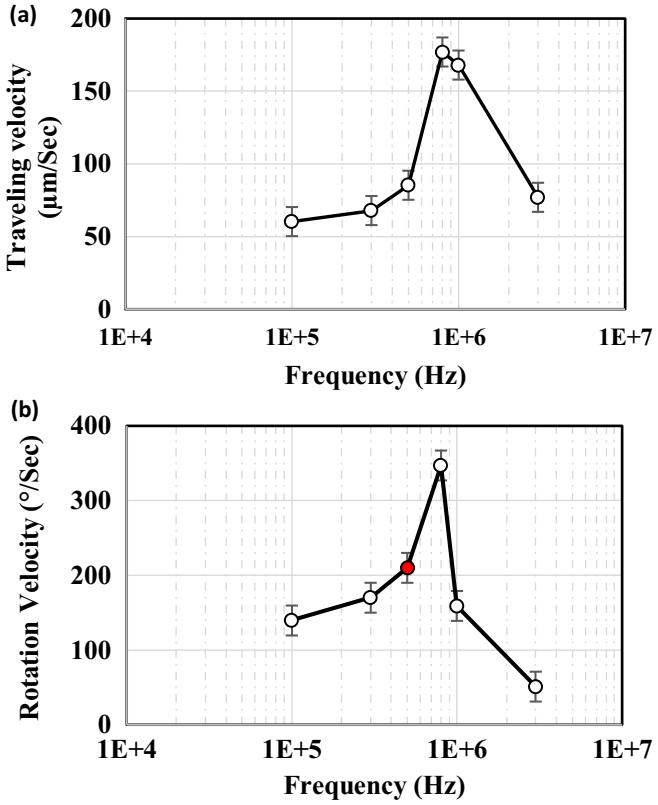

Fig. 10. Experimental results using square wave signal: a) The traveling wave velocity, and b) The Angular velocity of anticlockwise rotation 20 µm microbeads with respect to frequency. The Red point at (b) represent the clockwise rotation at this frequency. (For interpretation of the references to color in this figure legend, the reader is referred to the web version of this article.)

signal has a root mean square (RMS) value greater than the Sine wave. This simulation result is used to confirm the functionality of the proposed platform.

Table 2 presents the experimentally measured velocities of the microbeads under the effect of applying sinusoidal and square signals (the frequency of the applied signal is 800 KHz) for the three configurations (i.e., twDEP, levDEP, and rotDEP). It can be noticed that the velocities under the effect of square wave are higher compared to sinusoidal signals.

Both simulation and experimental results show the ability of the proposed electro-kinetic platform to be used in manipulating microbeads according to the following observations:

1- All the targeted DEP force configurations are fulfilled. For example, Fig. 7 shows the twDEP capability of the proposed platform. While, Fig. 8 shows the rotDEP capability of the platform. Fig. 9 presents the levDEP configuration, where the microbeads are trapped in the middle of the quadruple electrodes and then they are levitated. Levitation is observed when microbeads seem to be out of focus of the microscope and their color turn lighter compared to the non-levitated beads.
2- To prevent the burning of the electrodes, the proposed platform is used for a frequency range greater than 100 KHz without using any passivation layer on the top of it. This frequency (i.e., 100 KHz) is selected after many trials with different frequencies.
3- The square wave signal show greater DEP force compared to the sinusoidal signal. Consequently, the DEP velocity is greater when applying square wave signal. For example, Fig. 11, and Table 2 show a comparison between the DEP speed when applying sinusoidal and square wave signals, respectively.

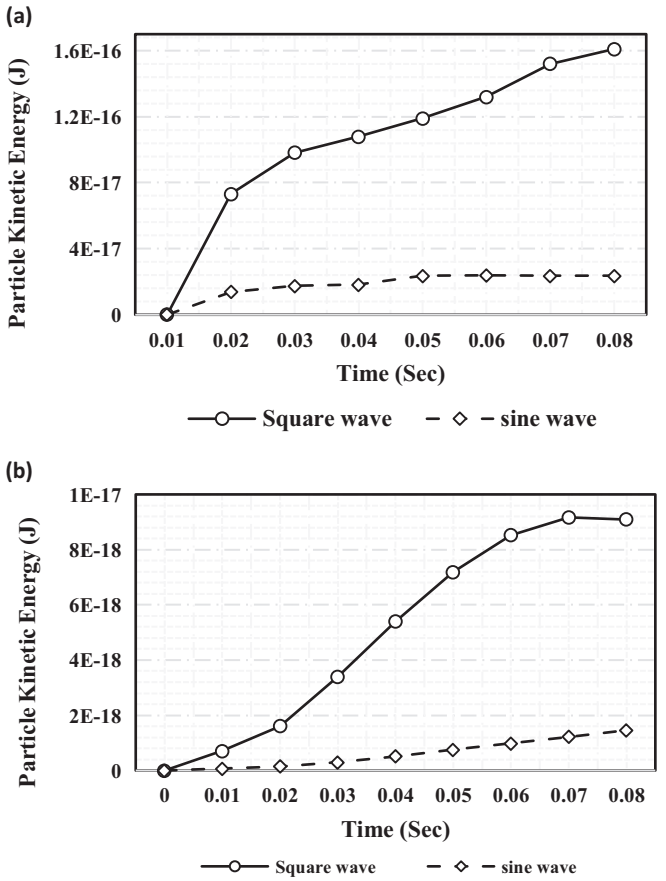

Fig. 11. A comparison between applying sine wave and square wave in the induced particles' kinetic energy: a) levDEp configuration. b) twDEP configuration.

Table 2
variation of the velocity between ac sine wave electrical and ac square electrical potential in case of traveling and levitation.

Electro-kinetic module\signal	Sine wave	Square wave
Traveling Velocity (μm/Sec)	103	177
Levitation Velocity (μm/Sec)	48	166
Rotation Velocity (°/Sec)	162	347

Table 3
Estimated capacitance of microbeads.

Features	Value
Radius R (μm)	10
Medium conductivity σ_m (μS/cm) (deionized water)	5.5 [30]
First characteristic peak Frequency f_α (MHz)	0.8
Capacitance $C_{cm} = \frac{2\sigma_m}{f_\alpha R}$ [13](μf/cm^2)	0.01375

The proposed platform which combines three DEP force configurations (i.e., twDEP, rotDEP and levDEP) allow not only the extraction of the velocities, but also the extraction of other useful features which are very important for efficient characterization and separation. For example, Table 3 shows the extraction of different features, such as first peak speed and the capacitance. Based on the capacitance, the permittivity of the membrane of the biological cells can be extracted [13]. Also, the membrane capacitance feature plays an important role in estimation of the surface morphological features such as surface protein

Table 4
A comparison between the proposed technique and other works.

Feature	[8]	[15]	Proposed
Technology	CMOS	Custom fabrication	PCB
Waveform Type	Sine	Sine	Square
Peak to peak voltage	5 V	3 V	10 Volt
Frequency range	10 kHz to 5 MHz	500 Hz to 100 kHz	100 kHz to 3 MHz
Trace / pitch width	4-μm 12-μm	10 μm 10 μm	150-μm 450-μm
Sum of electrodes	40➔Tw 31➔ rot	150 Tw	28 ➔ Tw 31 ➔ rot
Types of DEP configurations	twDEP rotDEP levDEP	twDEP	twDEP rotDEP levDEP
Sample cells	NCI-H929	Micro-beads	Micro-beads
Particle size	20 μm	5 μm	20 μm
Traveling velocity at frequency	−0.5 μm/s 2 MHz	11.4 μm/s 5 kHz	110 μm/s 2 MHz
First characteristic peak frequency	200 kHz	–	800 kHz

[13].

Table 4 shows comparison between the proposed platform and other published results in [13,15]. The used fabrication technology in [13] is CMOS technology which provides many advantages, such as miniaturization and integration capabilities. While [15] used gold PCB technology for fabrication which includes complex and expensive fabrication steps compared to the standard PCB technology that is used in the proposed platform. The proposed platform includes three different configurations, similar to [13]. However, [15] has only one configuration, refer to Table 4 for a detail comparison with [13,15].

8. Conclusions

An electro-kinetic platform based on DEP phenomenon using PCB technology that combines traveling, electro-rotation and levitation configurations (twDEP, rotDEP, and levDEP) on the same platform is presented and discussed. A model of electro-kinetic platform (Traveling, and levitation configurations) using COMSOL is described. The experimental results show that the proposed electro-kinetic platform using PCB technology is capable of manipulate and characterize microbeads. Also, the simulation and the experimental results proved that the ac square wave signal is more efficient than the traditionally ac sine wave signal for generating DEP electric field for the three major configurations (twDEP, rotDEP, and levDEP). Moreover, the proposed platform can be used to extract other features, such as capacitance and permittivity. Finally, a comparison between the proposed platform and other published systems is provided and discussed.

Acknowledgements

This research was partially funded by Zewail City of Science and Technology, AUC, the STDF, Intel, Mentor Graphics, ITIDA, SRC, ASRT and MCIT.

References

[1] Y.H. Ghallab, W. Badawy, Lab-on-a-Chip: Techniques, Circuits and Biomedical Applications, Artech House, Norwood, MA, 2010.
[2] Barbaros Cetin, Dongqing Li, Review dielectrophoresis in microfluidics technology, Electrophoresis 32 (2011) 2410–2427.
[3] M. Bocchi, M. Lombardini, A. Faenza, L. Rambelli, L. Giulianelli, N. Pecorari, et al., Dielectrophoretic trapping in microwell for manipulation of single cells and small aggregates of particles, Biosens. Bioelectron. 24 (2009) 1177–1183.
[4] S. Burgarella, S. Merlo, B. Dell'Anna, G. Zarola, M. Bianchessi, A modular microfluidic platform for cells handling by dielectrophoresis, Microelectron. Eng. 87 (2010) 2124–2133.
[5] H.A. Pohl, H.A. Pohl, Dielectrophoresis: The Behavior of Neutral Matter in

Nonuniform Electric Fields, Cambridge University Press, Cambridge, 1978, p. 80.
[6] T.B. Jones, Basic theory of dielectrophoresis and electrorotation, IEEE Eng. Med. Biol. Magazine 22 (6) (2003) 33–42.
[7] S.I. Han, Y.D. Joo, K.H. Han, An electrorotation technique for measuring the dielectric properties of cells with simultaneous use of negative quadrupolar dielectrophoresis and electrorotation, Analyst 138 (5) (2013) 1529–1537.
[8] H. Morgan, A.G. Izquierdo, D. Bakewell, N.G. Green, A. Ramos, The dielectrophoretic and travelling wave forces generated by interdigitated electrode arrays: analytical solution using Fourier series, J. Phys. D. Appl. Phys. 34 (10) (2001) 1553.
[9] S. Bunthawin, J. Kongklaew, A. Tuantranont, K. Jaruwongrangsri, T. Maturos, Microchip electrode development for traveling wave dielectrophoresis of non-spherical cell suspensions, Engineering 4 (10) (2013) 88.
[10] I.F. Cheng, V.E. Froude, Y. Zhu, H.C. Chang, H.C. Chang, A continuous high-throughput bioparticle sorter based on 3D traveling-wave dielectrophoresis, Lab Chip 9 (22) (2009) 3193–3201.
[11] S.I. Han, Y.D. Joo, K.H. Han, An electrorotation technique for measuring the dielectric properties of cells with simultaneous use of negative quadrupolar dielectrophoresis and electrorotation, Analyst 138 (5) (2013) 1529–1537.
[12] L. Hartley, K.V. Kaler, J. Luo, R. Paul, Discrete planar electrode dielectrophoresis systems, Electrical and Computer Engineering. Engineering Innovation: Voyage of Discovery. IEEE 1997 Canadian Conference, 1 1997, pp. 185–192.
[13] E.G. Cen, C. Dalton, Y. Li, S. Adamia, L.M. Pilarski, K.V. Kaler, A combined dielectrophoresis, traveling wave dielectrophoresis and electrorotation microchip for the manipulation and characterization of human malignant cells, J. Microbiol. Methods 58 (3) (2004) 387–401.
[14] J. Chung, H.Y. Hwang, Y. Chen, T.Y. Lee, Microfluidic packaging of high-density CMOS electrode array for lab-on-a-chip applications, Sensors Actuators B Chem. 254 (2018) 542–550.
[15] E. Morganti, C. Collini, R. Cunaccia, A. Gianfelice, L. Odorizzi, A. Adami, L. Lorenzelli, E. Jacchetti, A. Podesta, C. Lenardi, P. Milani, A dielectrophoresis-based microdevice coated with nanostructured TiO2 for separation of particles and cells, Microfluid. Nanofluid. 10 (6) (2011) 1211–1221.
[16] S.M. Hasan, A. Khurma, AC dielectrophoresis using elliptic electrode geometry, J. Sens. 2011 (2011).
[17] L. Altomare, M. Borgatti, G. Medoro, N. Manaresi, M. Tartagni, R. Guerrieri, R. Gambari, Levitation and movement of human tumor cells using a printed circuit board device based on software-controlled dielectrophoresis, Biotechnol. Bioeng. 82 (4) (2003) 474–479.
[18] C.T. Ho, Z. Zhang, T. Kaya, The Entrapment and Rotation of Cells using Dielectrophoresis, the 2014 ASEE North Central Section Conference, American Society for Engineering Education, 2014.
[19] A. Schmitz, S. Wagner, R. Hahn, H. Uzun, C. Hebling, Stability of planar PEMFC in printed circuit board technology, J. Power Sources 127 (1) (2004) 197–205.
[20] Spherotech - Technical - Characteristics of Polystyrene Particles, Retrieved from: http://www.spherotech.com/particle.html.
[21] R. Abdelbaset, Y.H. Ghallab, H. Abdelhamid, Y. Ismail, A 2D model of different electrode shapes for traveling wave dielectrophoresis, Microelectronics (ICM), 2016 28th International Conference on, IEEE, 2016, December, pp. 257–260.
[22] R. Abdelbaset, Y.H. Ghallab, H. Abdelhamid, Y. Ismail, M.T. El-Wakad, A 3D model of quadrupole dielectrophoresis levitation, Circuits and Systems (MWSCAS), 2016 IEEE 59th International Midwest Symposium on, IEEE, 2016, October, pp. 1–4.
[23] R. Pethig, M.S. Talary, R.S. Lee, Enhancing traveling-wave dielectrophoresis with signal superposition, IEEE Eng. Med. Biol. Magazine 22 (6) (2003) 43–50.
[24] L.M. Fu, G.B. Lee, Y.H. Lin, R.J. Yang, Manipulation of microparticles using new modes of traveling wave dielectrophoretic force: numerical simulation and experiments, J. IEEE/ASME Trans. 9 (2) (2004) 377–383.
[25] Iniyan Soundappa Elango, Development of a Dielectrophoretic Chip for Single Cell Electrorotation, Diss. Arizona State University, 2012.
[26] P.B. Tchounwou, C.G. Yedjou, A.K. Patlolla, D.J. Sutton, Heavy metal toxicity and the environment, Molecular, Clinical and Environmental Toxicology, Springer, Basel, 2012, pp. 133–164.
[27] Tracker Video Analysis, v.5.0.6 [computer software]. Douglas Brown. http://physlets.org/tracker/.
[28] R. Abdelbaset, Y.H. Ghallab, H. Abdelhamid, Y. Ismail, A model of electro-kinetic platform based on printed circuit board technology for manipulation and detection of liver cancer cells, Int. J. Comput. Appl. 154 (2) (November 2016) 0975–8887 V.
[29] S. Ueda, Y. Miyawaki, J. Wang, T. Matsuoka, K. Taniguchi, Wireless on-chip microparticle manipulation using pulse-driven dielectrophoresis, IEICE Electr. Exp. 9 (1) (2012) 16–22.
[30] A. Boughriet, Z. Wu, H. McCann, L.E. Davis, The measurements of dielectric properties of liquids at microwave frequencies using open-ended coaxial probes, Proc. 1st World Congr. Ind. Process Tomography Buxton, Greater Manchester, Apr. 14–17, 1999, pp. 318–322.